A Geospatial Analysis of the Relationship Between Land Surface Temperature and Land Use/Land Cover Indices in Raiganj Municipality, West Bengal, India

Bapi Sarkar
Raiganj University https://orcid.org/0000-0003-1871-5250
Sribas Patra (Sribaspatra2013@gmail.com)
Ravenshaw University https://orcid.org/0000-0001-7289-4080

Research Article

Keywords: Land Surface Temperature (LST), Normalized Difference Vegetation Index (NDVI), Normalized Difference Water Index (NDWI), Normalized Difference Built-up Index (NDBI), Raiganj Municipality

Posted Date: March 28th, 2022

DOI: https://doi.org/10.21203/rs.3.rs-1497635/v1

Abstract

The current research focuses on estimating land surface temperature (LST) in Raiganj Municipality, India, with their relationships of different land use and land cover (LULC) indices such as Normalized difference vegetation index (NDVI), Normalized difference water index (NDWI), and normalized difference built-up index (NDBI). Data were pre-processing Using ERDAS Imagine 14 and Arc GIS 10.3 software for layer stacking, mosaicking and clipping of the Landsat images. The analysis was based on Landsat TM 5 and Landsat 8 OLI satellite images of 2001, 2011, and 2021.The study observed that the values of LST, and NDBI were increased by 0.9˚C, and 0.71 from 2001 to 2021. And the values of NDVI, and NDWI were decreased by -0.20, and − 0.34 from 2001 to 2011. High land surface temperature is primarily located on the buildup area and LST level is low significantly due to the presence of vegetation and water bodies. The result indicates relationship between LST and the LULC indices, while LST has a significant positive association with NDBI, while NDVI and NDWI have a moderate to strong negative correlation. The study also found that changing land surface temperature has a significant influence on the ecosystem and loss of green space.

Introduction

In a mixed urban environment, the concept of land surface temperature (LST) is utilized to interpret the changing land use/land cover (LULC) pattern (Guha et al., 2020b; Pal and Ziaul, 2017; Saha et al., 2021; Tran et al., 2017). LST was established in several major global cities (including Beijing, Columbus, Shanghai, Baltimore, Chicago, and others) to address a variety of environmental issues (Asgarian et al., 2015; Das and Das, 2020; Kuang et al., 2014; Mukherjee and Singh, 2020; O'Connor, 2003; Peng et al., 2020). The nature and distribution of LST are influenced by various types of LULC indices (Bindajam et al., 2020; Bokaie et al., 2016; Guha and Govil, 2020; Hua and Ping, 2018; Kafy et al., 2020). Vegetation index, built-up index, Bareness index, water index, and other normalized difference LULC indices were frequently utilized in recent LST related studies to quantify their impact on the changing environmental status of urban areas (Aboelnour et al., 2018; Gantumur et al., 2017; Ullah et al., 2019; Weng, 2009). The linear correlation analysis between the LST and LULC indices were discussed in cities all around the world, including some recent publications that looked at the statistical linear link between LST and a few other LULC indices for different research areas(Ferreira and Duarte, 2019; Mallick et al., 2012; Naserikia et al., 2019; Rasul and Ibrahim, 2017; Sekertekin et al., 2015; Zhao et al., 2017). The seasonal impacts of Ohio City's thermal conditions were demonstrated using simple regression analysis (Li & Zhou, 2019). The seasonal fluctuations in the LST-LULC indices relationship were estimated using a combination of statistical approaches. Seasonal research on the link between the LST and LULC indexes was done in Jaipur, Rajasthan (Guha et al., 2020a). In Beijing, China, a new model was used to depict the seasonal fluctuation in LST. The yearly and seasonal trends of LST in peninsular Spain were identified using a statistical model. In China's metropolitan areas, another study of LST and climatic components was conducted. In the cities of China, a periodic interpretation of LST with weather factors was done. In Beijing, China, the variance of LST and land connectivity was investigated using a special index(Hassan et al., 2021; T. Li et al., 2020). As a result, there was a lot of correlation analysis between the LST and LULC indices in the study. Every city in India has been affected by the ongoing phenomenon of large-scale land-use changes as a result of globalization(Chadchan and Shankar, 2012). Recent studies have discovered that a region's land use and land cover are rapidly changing, which has become a major environmental issue in India(Herold et al., 2016; Lambin et al., 2003). Ramachandra's research reveals that when the pace of urbanization increases, the land surface temperature changes(Aithal et al., 2019; Kumar A and Singh Hooda B, 2013; Rajeswari et al., 2021). In India, the temperature rose by 3 to 4 degrees Celsius between 1989 and 2010. The loss of green spaces, as well as changes in local climate and the establishment of UHI, are all possible consequences of rising temperatures. The rapid population increase in metropolitan areas creates pressure on the physical environment and its resources(Alberti, 2016; Mersal, 2016; Smyth and Royle, 2000). As a result, the land use pattern and surface land cover are rapidly changing. This type of situation is common in developing countries, including India. Environmental degradation is a product of population, energy, industrialization, and urbanization, not only of population growth(J. Chen, 2007; Y. C. Chen, 2018). The current research looks at the association between land surface temperature and different LULC indices, as well as evaluating the environmental impact of urbanization in terms of reduced green space and increased land surface temperature. The current study made use of statistical, geographical, and indicators to achieve its goals. Using RS and GIS technologies, Studies have been carried out on the link between various land use indices. To show the variance of LST and their relationships, the Normalized Difference Vegetation Index, Normalized Difference Built-Up Index, and Normalized Difference Water Index were developed. Land surface temperature monitoring and management would aid land use planning by bridging the knowledge gap between present and past conditions and mitigating environmental concerns.

Materials And Methods

Study Area

The Raiganj municipality is situated in the southwestern part of the Uttar Dinajpur district in West Bengal, India. The town received municipal status on August 15, 1951, and it is also known for the Raiganj wildlife sanctuary (popularly known as Kulik bird sanctuary).25°38′27.102″ North and 25°34′ 57.153″ North latitude, and 88°6′23.812″ East and 88°9′5.932″ East longitude, this region is located (Fig. 1). The municipality covers 10.75 square kilometers and is located 425 kilometers from Kolkata, the state capital. The city of Raiganj is split into 26 wards. According to Census India 2011, the Raiganj Municipality has a population of 183,612, with 96,388 males and 87,224 females, and is located 30 metres above sea level. With the massive economic expansion and urban agglomeration, the town is designated the district headquarters of Utter Dinajpur. Many people come here for various reasons, not just from the Raiganj block but also from the adjacent districts.

Remote Sensing Data

Landsat imaging is particularly beneficial for detecting land-use change because it assists large-scale landscape studies efficiently and the data is updated and available regularly (Xie et al., 2019). This study uses cloud-free multi-temporal and multi-spectral Landsat TM (Thematic Mapper) data from 2001 and 2011, as well as Landsat 8 OLI (Operational Land Imager) data from 2021. The USGS - United States Geological Survey (https://earthexplorer.usgs.gov) was used to collect data from orbiting satellites that looked at land use and land cover patterns. The satellite data specs are listed below

Table 1
Characteristic of Landsat satellite images used in the study area

Satellite	Sensor ID	Year	Acquisition date	Resolution	Path/row	Projection
Landsat 5	TM	2001	04-02-2001	30 m	139/42	UTM-WGS1984
Landsat 5	TM	2011	31-01-2011	30 m	139/42	UTM-WGS1984
Landsat 8	OLI_TIRS 1991	2021	11-02-2021	30 m	139/42	UTM-WGS1984
Source: USGS Earth Explorer						

Satellite Image Processing

LST is calculated using Landsat TM 5 band-6 and Landsat 8 OLI images bands 10 and 11. The NDVI is calculated using red band 3 for TM, and 4 for OLI, and near-infrared band 4 for TM, band 5 for OLI. The gathered Landsat data of two path/row series were mosaic using ERDAS Imagine 14, and Arc GIS 10.3 were used for others analysis and layout. To execute remote sensing-based indices and provide the required output, the pictures were georeferenced to the UTM 45° N WGS-84 datum. Calculating spatial indices and assessing and defining the link between LST and other land use indices are the two stages of the current study's strategy. The methodological procedure for the study has been summarized in the diagram below (Fig. 2).

The Derivation of Land Surface Temperature (LST)

Landsat TM 5 images for the years 2001 and 2011 and Landsat 8 OLI (Operational Land Imager) imagery for the year 2021 with 0% cloud cover were used to calculate the land surface temperature (LST) of the Raiganj urban area. Landsat TM 5 imagery gives 7 bands thermal bands while Landsat 8 OLI imagery provides 11 bands, with band 10 and band 11 being thermal bands (Equations 1 to 6). The following are the procedures involved in turning digital values into spectral radiance when calculating temperature from TM and OLI images:

Step 1: Landsat TM 5 band 6 digital values to spectral radiances conversion.

The following formula was used to convert band 6 digital values into radiance values (Lλ) (Landsat Project Science Office 2002) $\mathrm{L}\lambda = \frac{\mathrm{LMAX}\lambda - \mathrm{LMIN}\lambda}{\mathrm{QCALMAX} - \mathrm{QCALMIN}} \times (\mathrm{QCAL} - \mathrm{QCALMIN}) + \mathrm{LMIN}\lambda$ (1)

Here, Lλ is the atmospherically corrected cell value as the radiance, QCAL is the digital image value, LMINλ is the spectral radiance scaled to QCALMIN, LMAXλ is the spectral radiance scaled to QCALMAX, and QCALMIN is the minimum quantization calibration. The radiance pixel value (usually 1), and QCALMAX are the maximum values of quantized calibrated pixels (usually 255).Landsat8 OLI spectral radiances were converted from band 10 and 11 digital data.

The following formula was used to convert the Landsat OLI band 10 and 11 digital data.

$$\mathrm{L}\lambda = ML \times QCAL + AL$$

Where Lλ is the spectral radiance at the top of the atmosphere, ML denotes the radiance multi-band X, AL denotes the radiance add band X, QCAL denotes the quantized and calibrated standard product pixel value, and X denotes the band number.The band-specific multiplicative rescaling factor ML and the band-specific additive rescaling factor AL are obtained from the metadata file (MTL file).

Step 2: At-satellite brightness spectral radiance temperatures conversion, emissivity modifications were added to radiant temperature based on the land cover nature following (Artis and Carnahan ,1982).

$$T = \frac{K_2}{Ln\left(\frac{K_1}{L\lambda} + 1\right)} - 273 \cdot 15$$

3

Where T is the at-satellite brightness temperature in Kelvin (K), Lλ is the at-satellite radiance in W/(m2srμm), and K_1 and $K_2$are the thermal calibration constants in W/(m2sr μm), respectively. (For Landsat-5 TM,K_1= 607.76, K_2 = 1260.56 for band 6, and for Landsat 8 OLI,K_1 for band 10 and 11 is 774.8853 and 480.8883 respectively, and, K_2 for band 10 and 11 is 1321.0789 and 1201.1442 respectively. The metadata file provided the values for $K_2$and K_1. For better understanding, the thermal constant values for Landsat TM and Landsat OLI are converted from Kelvin (K) to degrees Celsius (°C) using the Eq. 0°C = 273.15K.

Step 3: Emissions from the ground surface are measured (E)

The temperature values derived above are compared to a black body. As a result, spectral emissivity (E) adjustments are required. These can be done according to the land cover type (Snyder et al. 1998) or by calculating the emissivity values for each pixel from the proportion of vegetation (Pv) data.

$$E = 0.004 * PV + 0.986$$

4

Where the proportion of vegetation (PV) can be calculated as:

$$P_V = \left\{\frac{\left(NDVI_{max} - NDVI_{min}\right)}{\left(NDVI_{max} - NDVI_{\min}\right)}\right\}^2$$

5

Step 4: Land surface temperature (LST). LST is calculated using the equation below.

$$\frac{BT}{1} + W * \left(\frac{BT}{P}\right) * Ln(E)$$

6

Where BT is the brightness temperature at the satellite, W is the wavelength of emitted radiance, P = h*c/s (1.438 10 – 2 m K), h is the Planck's constant (6.626 10–34 Js), s is the Boltzmann constant (1.38 10–23 J/K), and is the light velocity (2.998 10 8 m/s).

Retrieval of LULC Indices

The following method was used to determine the relationship between LST and several spatial indices such as NDVI (Normalized Difference Vegetation Index), NDWI (Normalized Difference Water Index), and NDBI (Normalized Difference Built-Up Index) of the studied area (Equations7 to 9).

Calculation of Normalized Difference Vegetation Index (NDVI)

The NDVI value was extracted using the (Townshend and Justice, 1986) approach.

$$NDVI = \frac{(\mathrm{NIRband} - \mathrm{Rband})}{(\mathrm{NIRband} + \mathrm{Rband})}$$

7

Where NIR is the near-infrared band's DN (digital number) value and R is the red band's DN value. The NDVI value is a number that runs from 0 to 1. Low vegetation cover is indicated by values close to 0, and high vegetation density is indicated by values close to 1.

Calculation ofNormalized Difference Water Index (NDWI)

$$NDWI = \frac{(Greenband - NIRband)}{(\mathrm{Greenband} - \mathrm{NIRband})}$$

8

To avoid the problem of the built-up area being included in the NIR band, NDWI is used (Gu et al. 2008), $\sum$where green refers to the green band and NIR refers to the near-infrared band.

Calculation of Normalized Difference Built-up Index (NDBI)

The following formula (Zha et al. 2003) is used to calculate NDBI, with a value closer to 1 indicating a high density of built-up land.

$$NDBI = \frac{(\mathrm{MIRband} - \mathrm{NIRband})}{(\mathrm{MIRband} + \mathrm{NIRband})}$$

9

Where MIR is the DN from the mid-infrared band and NIR is the near-infrared band.

Pearson’s product-moment correlation coefficient (r)and Linear Regression method used ((Patra and Gavsker, 2021))

$$r = \frac{n(\sum xy) - (\sum x)(\sum y)}{\sqrt{[n\sum x^2 - \left(\sum x\right)^2\Big][n\sum y^2 - (\sum y)^2]}}$$

10

$$ {y}_{i}=\beta +{\beta }^{1}x{}^{1}+{\beta }^{2}x{}^{2}+\dots +\beta x+Ɛ $$

11

where, for i = n observations,

y_i = dependent variable,

x_i = expanatory variables,

β_0 = y-intercept (constant term),

β_p = slope coefficients for each explanatoryvariable,

ϵ = the model’s error term (also known as the

Output maps were created after the values of several spatial indices were calculated to depict the geographic distribution of vegetation cover, water coverage, and built-up areas throughout time.

Result And Discussion

The pattern of LST distribution among several LULC indices, such as vegetation cover, water covering, and built-up areas. The values measured from selected sample points across the region are used in regression analysis to show the link between LST and spatial indices. The correlation is calculated by fitting the trend line with Microsoft Excel and calculating the slopes of regression lines.

Spatio-temporal Distribution Land Surface Temperature Distribution (LST)

Year	2001	2011	2021
Maximum	22.821	21.066	23.717
Minimum	17.023	16.565	19.382
Mean	19.465	18.527	21.680
SD	0.967	0.544	0.548

Land surface temperature distribution maps for the Raiganj Municipality area have been created over time to show how the LST distribution has changed (Fig. 3). The results show that LST values have risen through different time period of the city. The lowest radiant temperature in 2001 was 16.50-18.40 °C covering an area of 2.02 Sq.km areas covert and 17.77 percentage of the total area. The highest radiant temperature in 2001 was 22.23-24.13°C covering an area of 1.96 Sq.km areas covert and 17.31 percentage of the total area. Moderately low to moderately high temperature in 2001 is 18.41-22.22°C covering an area 7.37sq.km and 64.92 percent area cover of total area. The lowest radiant temperature in 2011 was 16.50-18.40 °C covering an area of 1.88 sq.km area covert and 16.56 percentage of the total area. The highest radiant temperature in 2011 was 22.23-24.13 °C covering an area of 2.02 Sq.km areas covert and 17.80 percentage of the total area. Moderately low to moderately high temperature in 2011 is 18.41-22.22°C covering an area 7.45sq.km and 65.64 percent area cover of total area. The lowest radiant temperature in 2021 was 16.50-18.40 °C covering an area of 1.05 sq.km area covert and 9.24 percentage of the total area. The highest radiant temperature in 2021 was 22.23-24.13 °C covering an area of 2.46 Sq.km areas covert and 21.67 percentage of the total area. Moderately low to moderately high temperature in 2021 is 18.41-22.22°C covering an area 7.845sq.km and 69.08 percent area cover of total area(Table 3) .LST has changed over time in different land-use units from 2001 to 2021. LST has grown significantly over each land cover unit, particularly built-up land, sand deposition, and water body area Over 20 years (Table 3).

Table 2 Descriptive statistics of Land surface temperature of different temporal periods.

Category	Tem˚ C	Years					
		2001		2011		2021	
		Area(sq.km	Percentage	Area(sq.km)	Parentage	Area(sq.km)	Percentage
Low	16.50–18.40	2.02	17.77	1.88	16.56	1.05	9.24
Moderately Low	18.41–20.31	4.77	41.99	4.71	41.53	3.60	31.73
Moderately High	20.32–22.22	2.60	22.93	2.74	24.11	4.24	37.35
High	22.23–24.13	1.96	17.31	2.02	17.80	2.46	21.67
Total	11.35		100	11.35	100	11.35	100

Analysis of Spatial Characteristics of NDVI, NDBI, and NDWI

In the years 2001, 2011, and 2021 show the NDVI, NDBI, and NDWI were used to create maps and statistics over different periods. The relative dispersion of measured spatial indices for each research year has been depicted using the coefficient of variation (CV). Descriptive statistics show for NDVI, NDWI, and NDBI during periods. For the years 2001, 2011, and 2021 NDVI was used to create vegetation cover maps (Fig. 4). Within the urban region, there is a notable decrease in vegetation growth coverage (scattered vegetation and woodland). Water body areas have lower NDVI values as well. In 2001 the highest NDVI value is 0.466 and in 2021 the highest NDVI is 0.264 it means decreasing the growth of vegetation as well as increasing urban growth (Table 3).

NDWI pattern of the year 2001, 2011, and 2021 has been extracted by using the NDWI index (Fig. 5). There is a significant change in the coverage of the water bodies as the maximum NDWI value decreases from 0.56 in 2001 to 0.22 in 2021.The concentration is highest NDWI is water body area and lowest concentration in build-up area. At some level, the presence of water bodies aids in lowering its own as well as the surrounding temperature (Table 3).

Figure 5 Spatial distribution of NDWI of 2001, 2011 and 2021.

Built-up maps are created by visualizing the area's built-up growth (Fig. 6) using the NDBI (Normalized Difference Built-up Index). Built-up and unoccupied land in densely populated areas has high NDBI values. Due to land conversion to developed land with industrial and commercial buildings, residential buildings, roads, and transportation communication, the maximum NDBI value significantly rose. As a result, high NDBI values can be seen in built-up areas and other impermeable surfaces, whereas low NDBI values can be seen over water bodies and vegetation cover (Table 3).

Table 4
The Statistical Description of NDVI, NDWI, and NDBI in study years.

LULC indices	YEAR	2001	2011	2021
NDVI	Minimum	-0.31	-0.123	-0.027
	Maximum	0.466	0.171	0.264
	Mean	0.146	0.005	0.089
	SD	0.087	0.033	0.035
NDWI	Minimum	-0.405	-0.494	-0.117
	Maximum	0.565	0.25	0.224
	Mean	-0.137	-0.109	0.050
	SD	0.110	0.083	0.046
NDBI	Minimum	-0.565	-0.25	-0.224
	Maximum	0.405	0.494	1.117
	Mean	0.137	0.109	-0.050
	SD	0.110	0.083	0.046

Source: Compiled by authors

Figure 6 Spatial distribution of NDBI of 2001, 2011 and 2021.

Correlation between LST and LULC Indices

Sample points collected of the study area of research years within the planning territory were measured to determine the link between LST and LULC indices. The retrieved values of the selected parameters (LST, NDVI, NDWI, and NDBI) are used to build a regression model. The association between LST and various LULC indices land was studied using a linear regression model for each land use type separately. In the area where the R^2 (coefficient of determination) produced from the regression model is 0.394, 0.401, and 0.608 for the years 2001, 2011, and 2021, there is a strong negative connection (Fig. 7) between surface temperature and vegetation cover. The high R^2 value in 2021 demonstrated that vegetation plays an important impact in reducing surface radiative temperature (Fig. 7).

LST and NDWI have a negative connection, signifying lower temperatures in water body locations and higher temperatures in non-water body areas. The linear regression model revealed this association with an$R^2$are 0.379,0.4086, and 0.551 of the year’s 2001,2011,2021 respectively(Fig. 8).The higher R^2 value in 2021 shows that water bodies play an important impact in reducing surface radiative temperature (Fig. 5). The perfect positive relationship between LST and NDBI is seen in Fig. 7. In 2021, the R^2 value generated by the model was 0.6316, which is higher than in 2001. The fact that a rise in built-up or impermeable surface captured the radiation that positively controls LST was established by such a high value of R^2 (Fig. 7 and Fig. 8). As a result of the research, it was discovered that land surface temperature (LST) is sensitive to each land use type and may thus be used to identify changes in land use and land cover.

Conclusion

In this paper, Landsat TM 5 and Landsat 8 OLI for the different years have been used to investigate the dynamic relationship between LST with NDVI, NDWI, and NDBI and evaluate the environmental impact of urbanization in terms of reduced green space and increased land surface temperature, UHI intensity effect in the area. At the pixel level, the associations between LST and NDVI, NDWI, and NDBI have been quantified using linear regression analysis (using Pearson's product-moment correlation coefficient). LST has a significant positive association with NDBI for the whole Raiganj municipality and a moderate to strong negative correlation with NDVI and NDWI. There has been an obvious change in the spatial structure of land use to meet the planning region's dynamic growth. The land use pattern in Raiganj Municipality areas is changing faster as a result of the fast population increase. A large amount of light vegetation and agricultural land has been cleared, and open spaces and wetlands have been converted into development property. The study shows that the radiative surface temperature is regulated by green space,the distribution of the UHI is significantly influenced by plant cover in the urban area. UHIs have been identified through the spatial distribution of LST which are mainly existed in bare land and built-up area, this area mostly responsible for generating high LST values of the city. LST level is reduced significantly due to the presence of vegetation and water bodies. The study found that changing land cover has a significant influence in terms of land surface temperature and loss of green area, the ecosystem is suffering. Many more research works may be included in the future. To begin, other satellite data of various spatial resolutions (e.g., IKONOS (1 m), Quickbird (0.6 m), ASTER (15 m), Sentinel-2A (10 m), MODIS (1000 m), etc can be used to carry out the full research project.

Declarations

Conflicts of Interest The authors declare no conflict of Interest

Acknowledgments The authors acknowledge the United State Geological Survey (USGS), Earth explorer for providing the free of cost satellite data of the study area.

References

1. Aboelnour M., Engel B.A., Aboelnour M. and Engel B.A. (2018). Application of Remote Sensing Techniques and Geographic Information Systems to Analyze Land Surface Temperature in Response to Land Use/Land Cover Change in Greater Cairo Region, Egypt. Journal of Geographic Information System, 10(1), 57–88. DOI: 10.4236/JGIS.2018.101003
2. Aithal B.H., Chandan M.C. and Nimish G. (2019). *Assessing land surface temperature and land use change through spatio-temporal analysis: a case study of select major cities of India*. 1–16.
3. Alberti M. (2016). Modeling the Urban Ecosystem: A Conceptual Framework: Https://Doi.Org/10.1068/B260605, 26(4), 605–630. DOI: 10.1068/B260605
4. Asgarian A., Amiri B.J. and Sakieh Y. (2015). Assessing the effect of green cover spatial patterns on urban land surface temperature using landscape metrics approach. Urban Ecosystems, 18(1), 209–222. DOI:

10.1007/S11252-014-0387-7

5. Bindajam A.A., Mallick J., AlQadhi S., Singh C.K. and Hang H.T. (2020). Impacts of vegetation and topography on land surface temperature variability over the semi-arid mountain cities of Saudi Arabia. Atmosphere, 11(7), 1–28. DOI: 10.3390/ATMOS11070762
6. Bokaie M., Zarkesh M.K., Arasteh P.D. and Hosseini A. (2016). Assessment of Urban Heat Island based on the relationship between land surface temperature and Land Use/ Land Cover in Tehran. Sustainable Cities and Society, 23, 94–104. DOI: 10.1016/j.scs.2016.03.009
7. Chadchan J. and Shankar R. (2012). An analysis of urban growth trends in the post-economic reforms period in India. International Journal of Sustainable Built Environment, 1(1), 36–49. DOI: 10.1016/J.IJSBE.2012.05.001
8. Chen J. (2007). Rapid urbanization in China: A real challenge to soil protection and food security. CATENA, 69(1), 1–15. DOI: 10.1016/J.CATENA.2006.04.019
9. Chen Y.C. (2018). Effects of urbanization on municipal solid waste composition. Waste Management, 79, 828–836. DOI: 10.1016/J.WASMAN.2018.04.017
10. Das M. and Das A. (2020). Urban Climate Assessing the relationship between local climatic zones (LCZs) and land surface temperature (LST) – A case study of Sriniketan- Santiniketan Planning Area (SSPA), West Bengal, India. Urban Climate, 32(January), 100591. DOI: 10.1016/j.uclim.2020.100591
11. Ferreira L.S. and Duarte D.H.S. (2019). Exploring the relationship between urban form, land surface temperature and vegetation indices in a subtropical megacity. Urban Climate, 27, 105–123. DOI: 10.1016/J.UCLIM.2018.11.002
12. Gantumur B., Wu F., Zhao Y., Vandansambuu B., Dalaibaatar E., Itiritiphan F. and Shaimurat D. (2017). Implication of relationship between natural impacts and land use/land cover (LULC) changes of urban area in Mongolia. Https://Doi.Org/10.1117/12.2278360, 10431, 139–157. DOI: 10.1117/12.2278360
13. Guha S. and Govil H. (2020). Seasonal impact on the relationship between land surface temperature and normalized difference vegetation index in an urban landscape. Https://Doi.Org/10.1080/10106049.2020.1815867. DOI: 10.1080/10106049.2020.1815867
14. Guha S., Govil H., Gill N. and Dey A. (2020a). Analytical study on the relationship between land surface temperature and land use/land cover indices. Annals of GIS, 26(2), 201–216. DOI: 10.1080/19475683.2020.1754291
15. Guha S., Govil H., Gill N. and Dey A. (2020b). Annals of GIS Analytical study on the relationship between land surface temperature and land use / land cover indices. Annals of GIS, 26(2), 201–216. DOI: 10.1080/19475683.2020.1754291
16. Hassan T., Zhang J., Prodhan F.A., Pangali Sharma T.P. and Bashir B. (2021). Surface urban heat islands dynamics in response to lulc and vegetation across south asia (2000–2019). Remote Sensing, 13(16), 1–24. DOI: 10.3390/rs13163177
17. Herold M., Scepan J. and Clarke K.C. (2016). The Use of Remote Sensing and Landscape Metrics to Describe Structures and Changes in Urban Land Uses: Http://Dx.Doi.Org/10.1068/A3496, 34(8), 1443–1458. DOI: 10.1068/A3496
18. Hua A.K. and Ping O.W. (2018). The influence of land-use/land-cover changes on land surface temperature: a case study of Kuala Lumpur metropolitan city. Https://Doi.Org/10.1080/22797254.2018.1542976, 51(1), 1049–1069. DOI: 10.1080/22797254.2018.1542976

19. Kafy A. Al, Rahman M.S., Faisal A. Al, Hasan M.M. and Islam M. (2020). Modelling future land use land cover changes and their impacts on land surface temperatures in Rajshahi, Bangladesh. Remote Sensing Applications: Society and Environment, 18, 100314. DOI: 10.1016/J.RSASE.2020.100314
20. Kuang W., Liu Y., Dou Y., Chi W., Chen G., Gao C., Yang T., Liu J. and Zhang R. (2014). What are hot and what are not in an urban landscape: quantifying and explaining the land surface temperature pattern in Beijing, China. Landscape Ecology 2014 30:2, 30(2), 357–373. DOI: 10.1007/S10980-014-0128-6
21. Kumar A S. and Singh Hooda B R. (2013). *Monitoring and prediction of land use land cover changes and its impact on land surface temperature in the central part of hisar district, haryana under semi-arid zone of india*. 125(11), 122001. DOI: 10.2478/jlecol-2019-0020
22. Lambin E.F., Geist H.J. and Lepers E. (2003). Dynamics of Land-Use and Land-Cover Change in Tropical Regions. Https://Doi.Org/10.1146/Annurev.Energy.28.050302.105459, 28, 205–241. DOI: 10.1146/ANNUREV.ENERGY.28.050302.105459
23. Li T., Cao J., Xu M., Wu Q. and Yao L. (2020). The influence of urban spatial pattern on land surface temperature for different functional zones. Landscape and Ecological Engineering, 16(3), 249–262. DOI: 10.1007/s11355-020-00417-8
24. Li X. and Zhou W. (2019). Optimizing urban greenspace spatial pattern to mitigate urban heat island effects: Extending understanding from local to the city scale. Urban Forestry and Urban Greening, 41, 255–263. DOI: 10.1016/j.ufug.2019.04.008
25. Mallick J., Singh C.K., Shashtri S., Rahman A. and Mukherjee S. (2012). Land surface emissivity retrieval based on moisture index from LANDSAT TM satellite data over heterogeneous surfaces of Delhi city. International Journal of Applied Earth Observation and Geoinformation, 19(1), 348–358. DOI: 10.1016/J.JAG.2012.06.002
26. Mersal A. (2016). Sustainable Urban Futures: Environmental Planning for Sustainable Urban Development. Procedia Environmental Sciences, 34, 49–61. DOI: 10.1016/J.PROENV.2016.04.005
27. Mukherjee F. and Singh D. (2020). Assessing Land Use–Land Cover Change and Its Impact on Land Surface Temperature Using LANDSAT Data: A Comparison of Two Urban Areas in India. Earth Systems and Environment 2020 4:2, 4(2), 385–407. DOI: 10.1007/S41748-020-00155-9
28. Naserikia M., Shamsabadi E.A., Rafieian M. and Filho W.L. (2019). The urban heat island in an urban context: A case study of Mashhad, Iran. International Journal of Environmental Research and Public Health, 16(3). DOI: 10.3390/ijerph16030313
29. O'Connor K. (2003). Global air travel: Toward concentration or dispersal? Journal of Transport Geography, 11(2), 83–92. DOI: 10.1016/S0966-6923(03)00002-4
30. Pal S. and Ziaul S. (2017). Detection of land use and land cover change and land surface temperature in English Bazar urban centre. Egyptian Journal of Remote Sensing and Space Science, 20(1), 125–145. DOI: 10.1016/j.ejrs.2016.11.003
31. Patra S. and Gavsker K.K. (2021). Land use and land cover change-induced landscape dynamics: A geospatial study of Durgapur Sub-Division, West Bengal (India). Acta Universitatis Carolinae, Geographica, 56(1), 79–94. DOI: 10.14712/23361980.2021.3
32. Peng X., Wu W., Zheng Y., Sun J., Hu T. and Wang P. (2020). Correlation analysis of land surface temperature and topographic elements in Hangzhou, China. Scientific Reports 2020 10:1, 10(1), 1–16. DOI: 10.1038/s41598-020-67423-6

33. Rajeswari J.R., Srinivas C. V., Yesubabu V., Hari Prasad D. and Venkatraman B. (2021). Impacts of Urbanization, Aerodynamic Roughness, and Land Surface Processes on the Extreme Heavy Rainfall Over Chennai, India. Journal of Geophysical Research: Atmospheres, 126(10). DOI: 10.1029/2020JD034017
34. Rasul G. and Ibrahim F. (2017). *Urban Land Use Land Cover Changes and Their Effect on Land Surface Temperature: Case Study Using Dohuk City in the Kurdistan Region of Iraq*. DOI: 10.3390/cli5010013
35. Saha S., Saha A., Das M., Saha A., Sarkar R. and Das A. (2021). Analyzing spatial relationship between land use/land cover (LULC) and land surface temperature (LST) of three urban agglomerations (UAs) of Eastern India. Remote Sensing Applications: Society and Environment, 22(April), 100507. DOI: 10.1016/j.rsase.2021.100507
36. Sekertekin A., Kutoglu S.H. and Kaya S. (2015). Evaluation of spatio-temporal variability in Land Surface Temperature: A case study of Zonguldak, Turkey. Environmental Monitoring and Assessment 2015 188:1, 188(1), 1–15. DOI: 10.1007/S10661-015-5032-2
37. Smyth C.G. and Royle S.A. (2000). Urban landslide hazards: incidence and causative factors in Niterói, Rio de Janeiro State, Brazil. Applied Geography, 20(2), 95–118. DOI: 10.1016/S0143-6228(00)00004-7
38. Tran D.X., Pla F., Latorre-carmona P., Myint S.W., Caetano M. and Kieu H. V. (2017). ISPRS Journal of Photogrammetry and Remote Sensing Characterizing the relationship between land use land cover change and land surface temperature. ISPRS Journal of Photogrammetry and Remote Sensing, 124, 119–132. DOI: 10.1016/j.isprsjprs.2017.01.001
39. Ullah S., Ahmad K., Sajjad R.U., Abbasi A.M., Nazeer A. and Tahir A.A. (2019). Analysis and simulation of land cover changes and their impacts on land surface temperature in a lower Himalayan region. Journal of Environmental Management, 245, 348–357. DOI: 10.1016/J.JENVMAN.2019.05.063
40. Weng Q. (2009). Thermal infrared remote sensing for urban climate and environmental studies: Methods, applications, and trends. ISPRS Journal of Photogrammetry and Remote Sensing, 64(4), 335–344. DOI: 10.1016/J.ISPRSJPRS.2009.03.007
41. Zhao Z.Q., He B.J., Li L.G., Wang H.B. and Darko A. (2017). Profile and concentric zonal analysis of relationships between land use/land cover and land surface temperature: Case study of Shenyang, China. Energy and Buildings, 155, 282–295. DOI: 10.1016/j.enbuild.2017.09.046

Figures

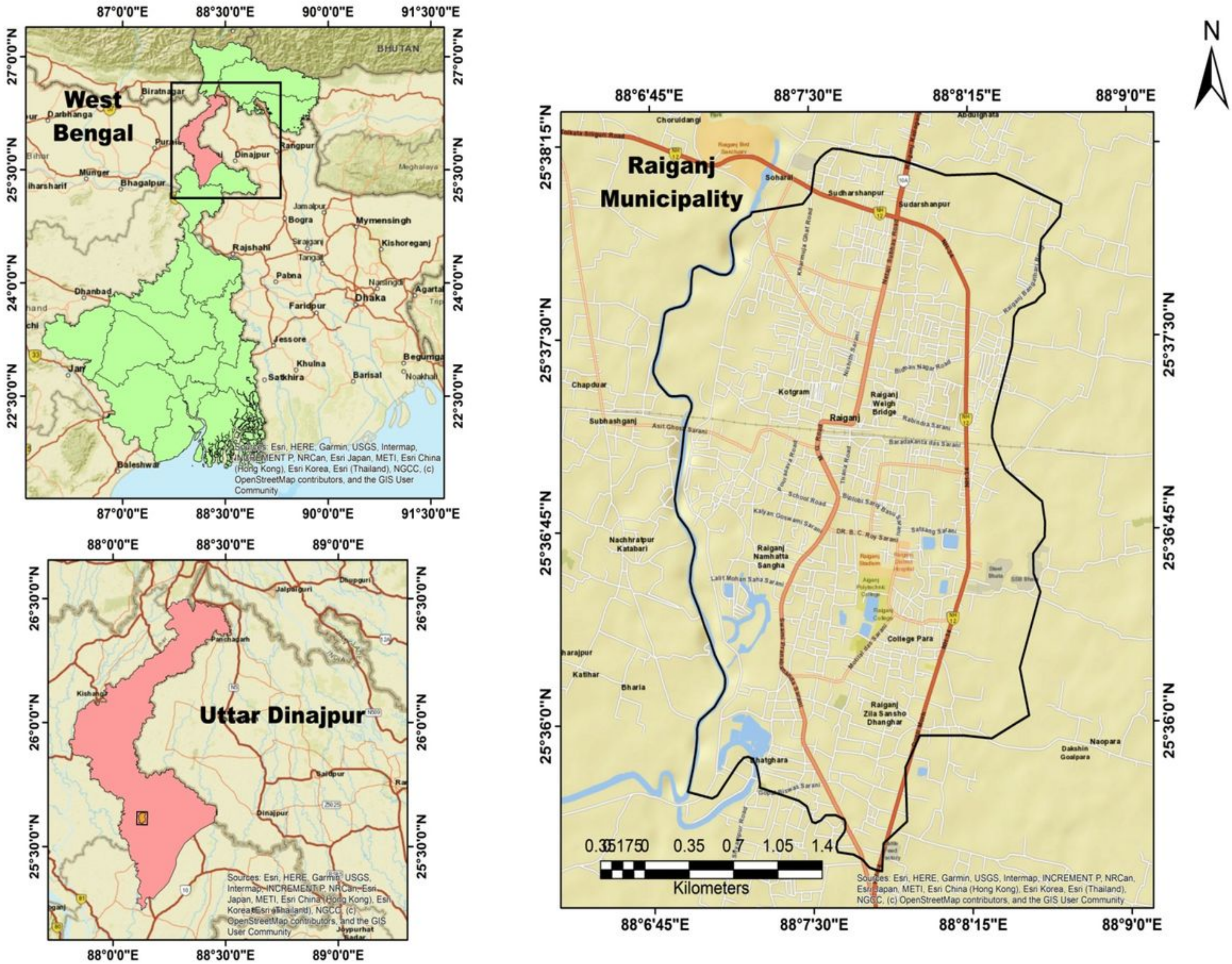

Figure 1

Location Map of the Study Area

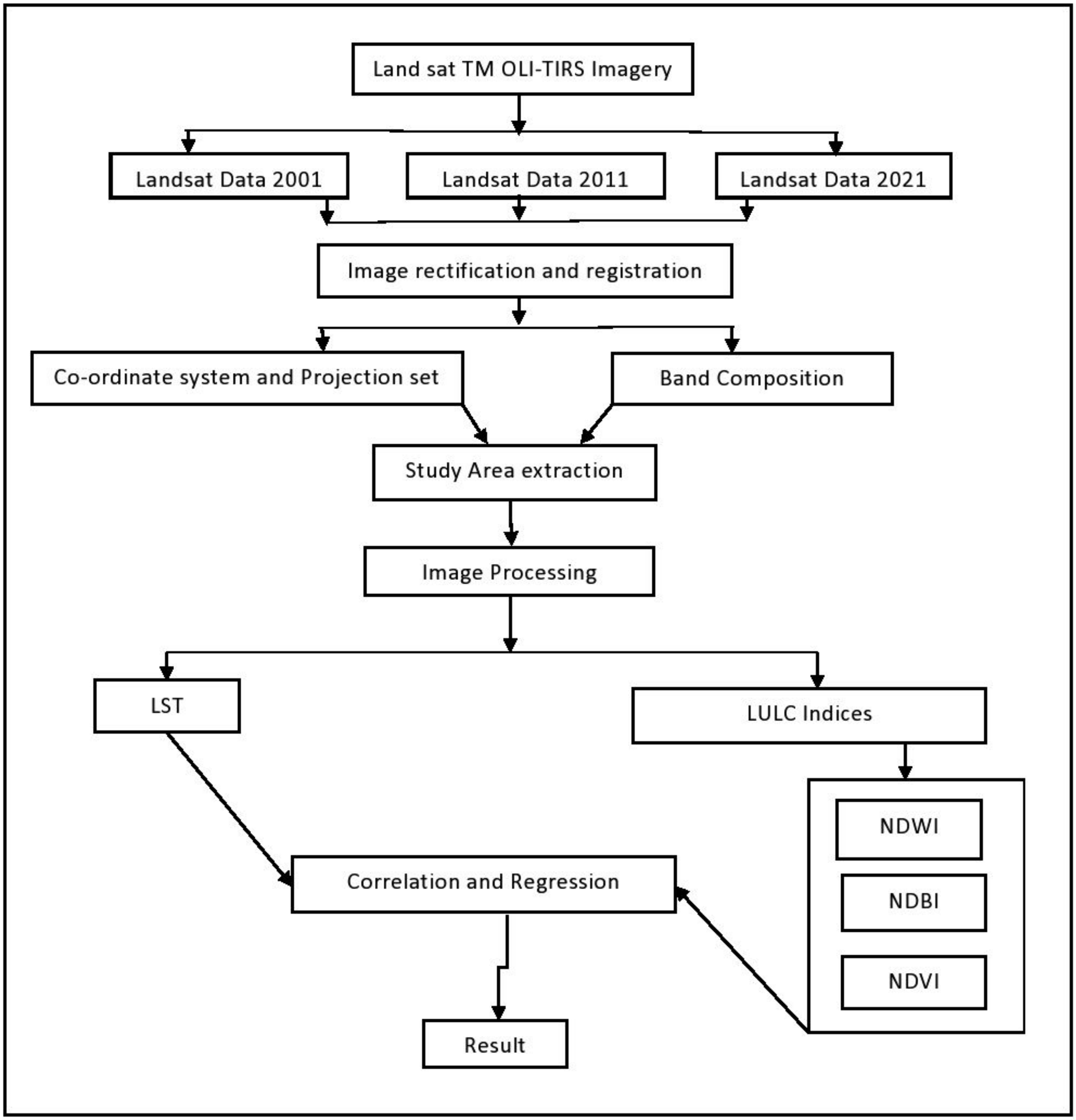

Figure 2

Methodology Chart

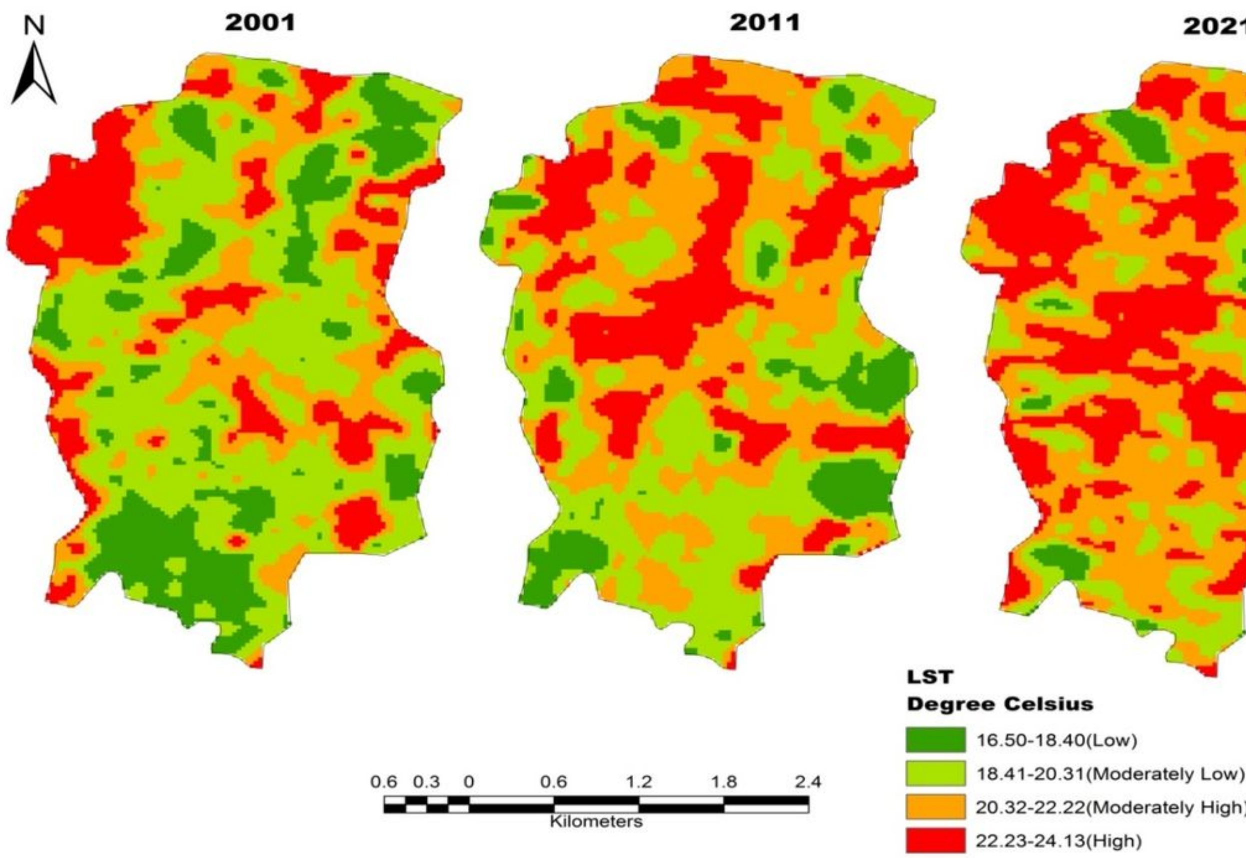

Figure 3

Spatial distribution of NDBI of 2001, 2011 and 2021.

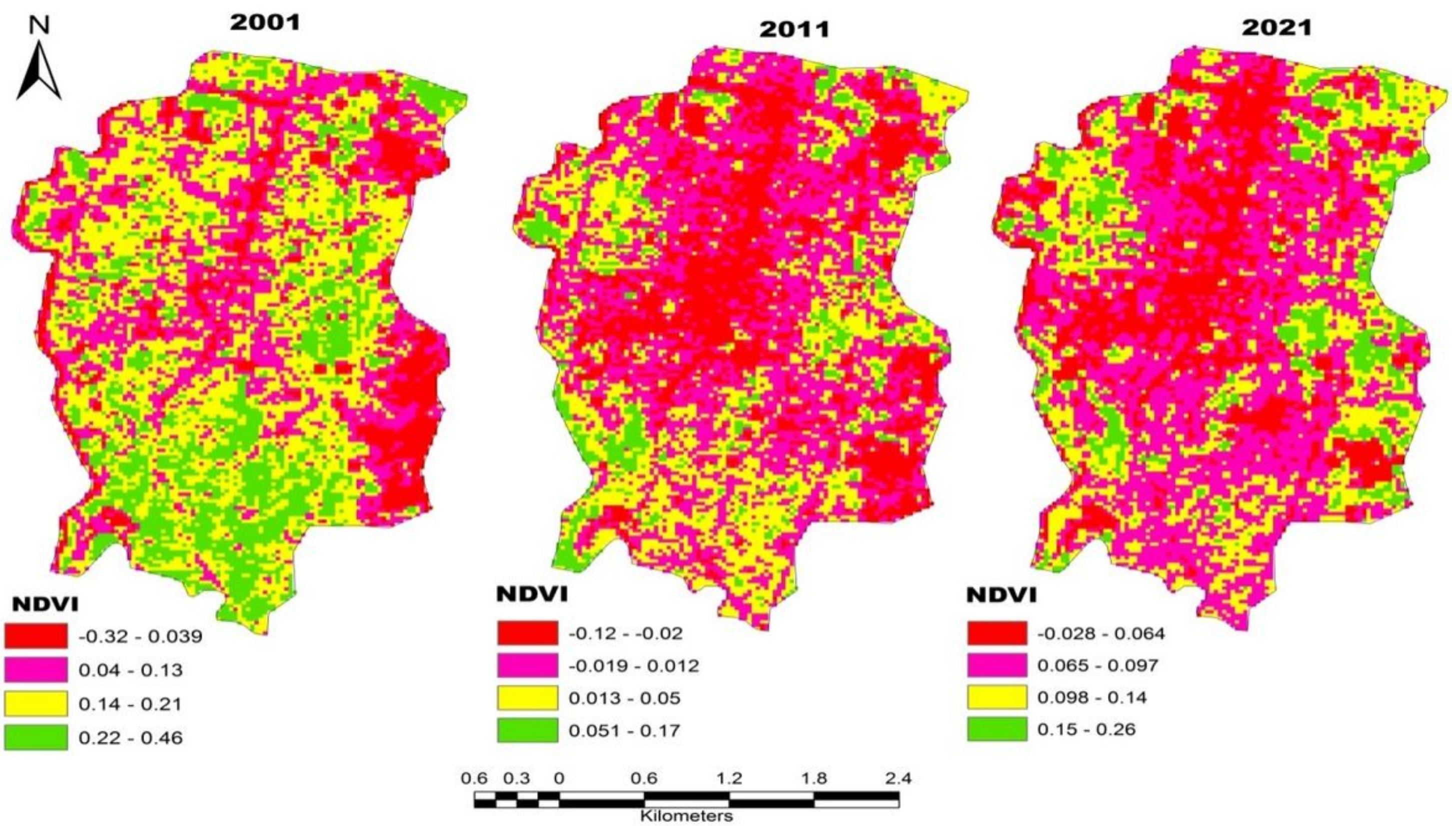

Figure 4

Spatial distribution of NDVI of 2001, 2011 and 2021.

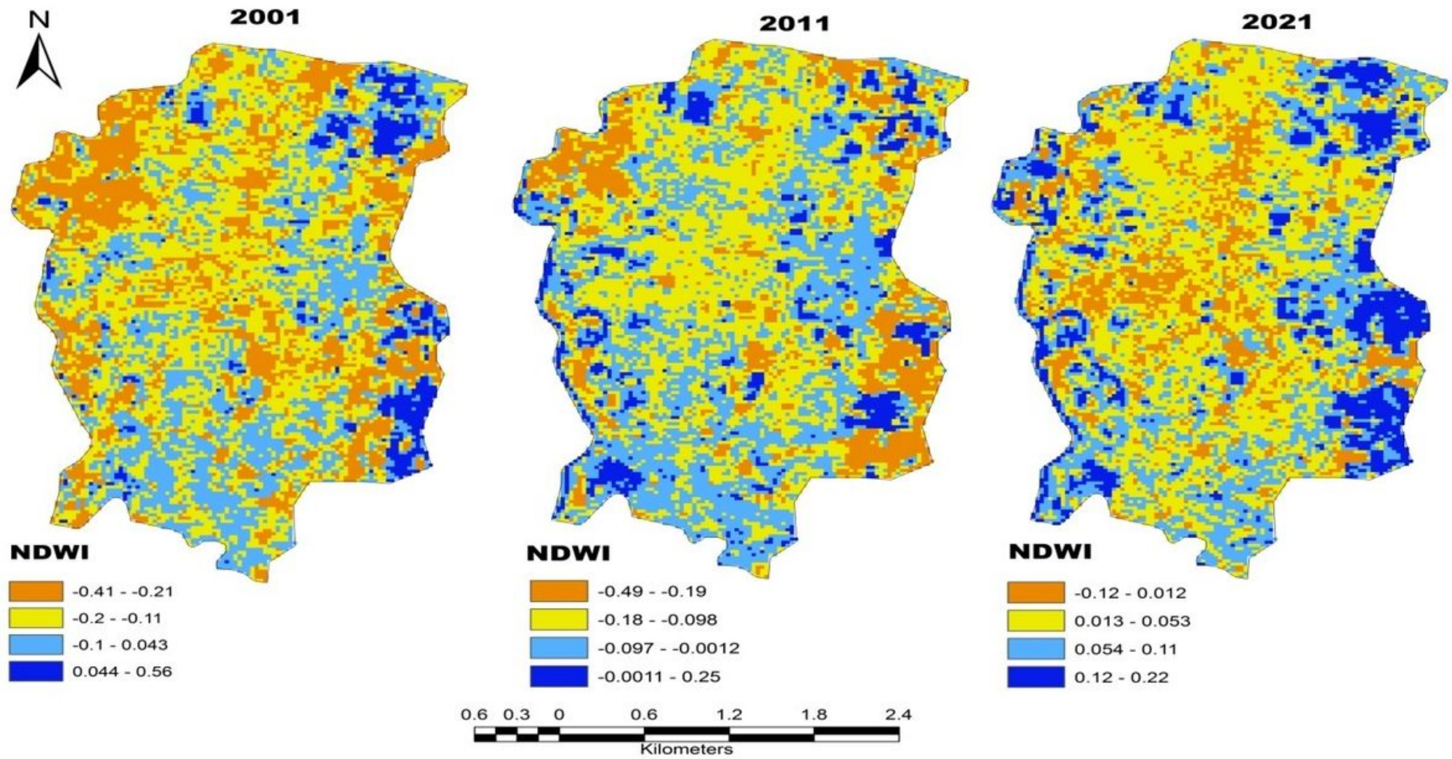

Figure 5

Spatial distribution of NDWI of 2001, 2011 and 2021.

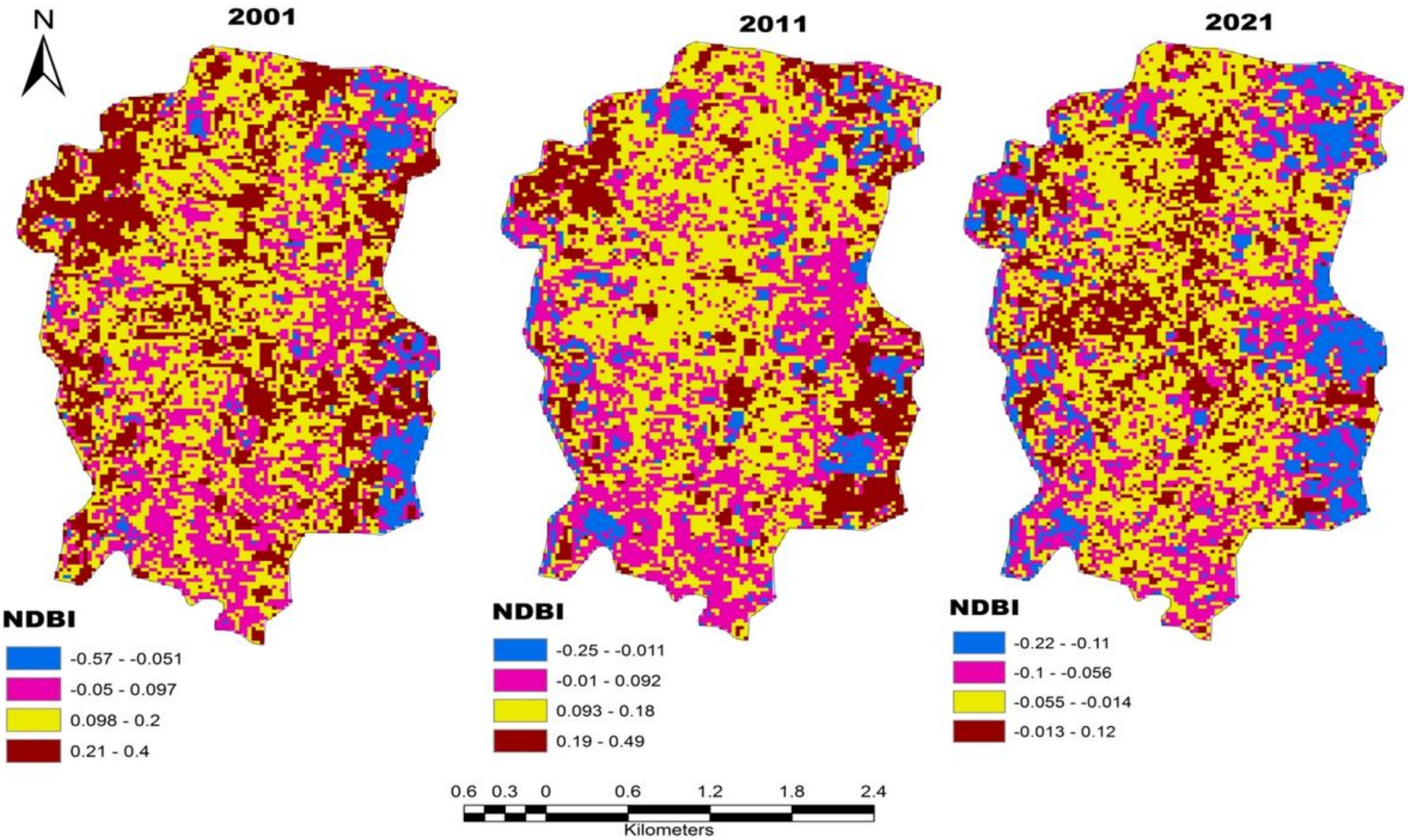

Figure 6

Spatial distribution of NDBI of 2001, 2011 and 2021.

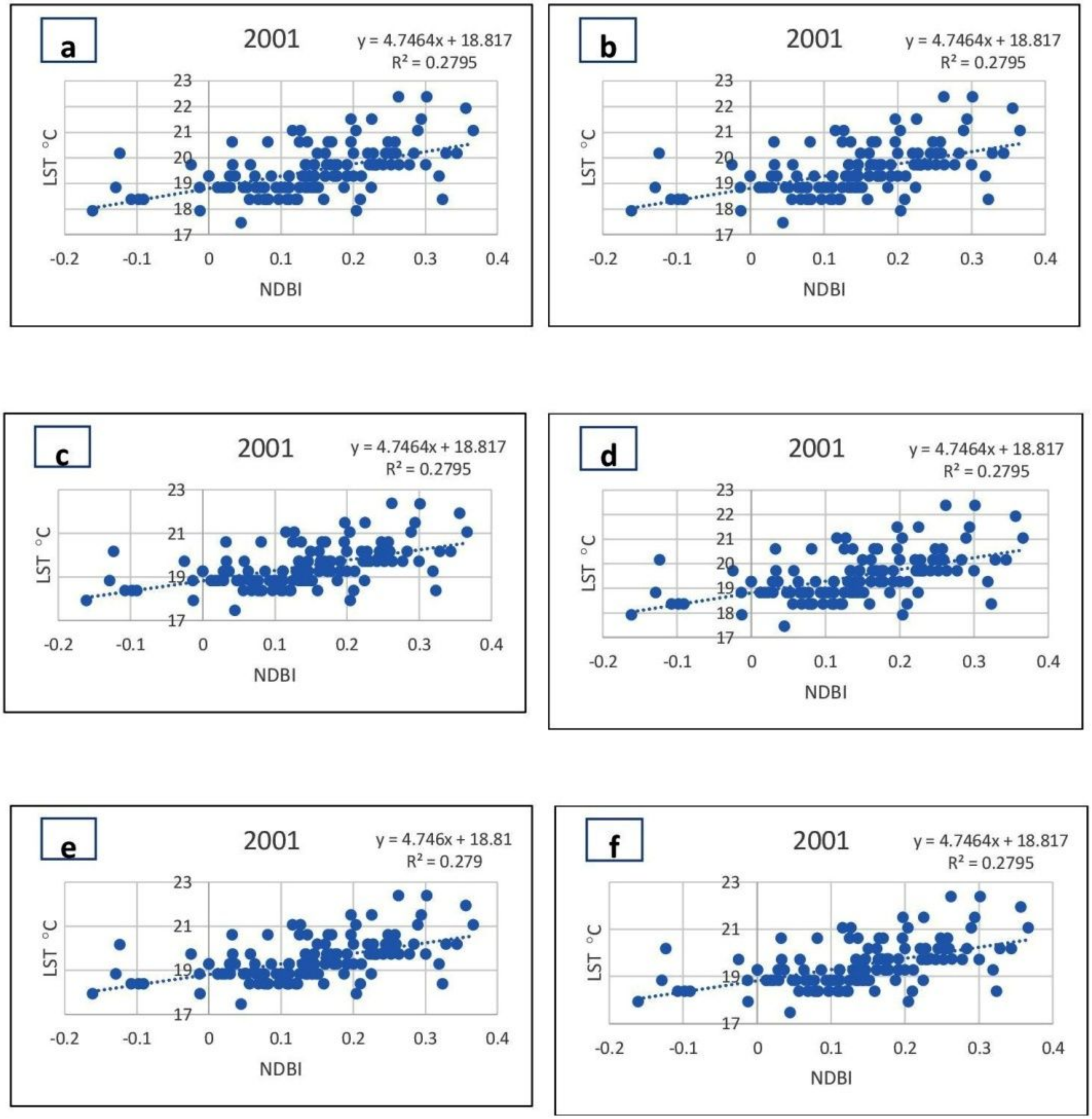

Figure 7

Regression correlation between LST and NDVI (a, c, and e); and NDBI (b, d, and f)

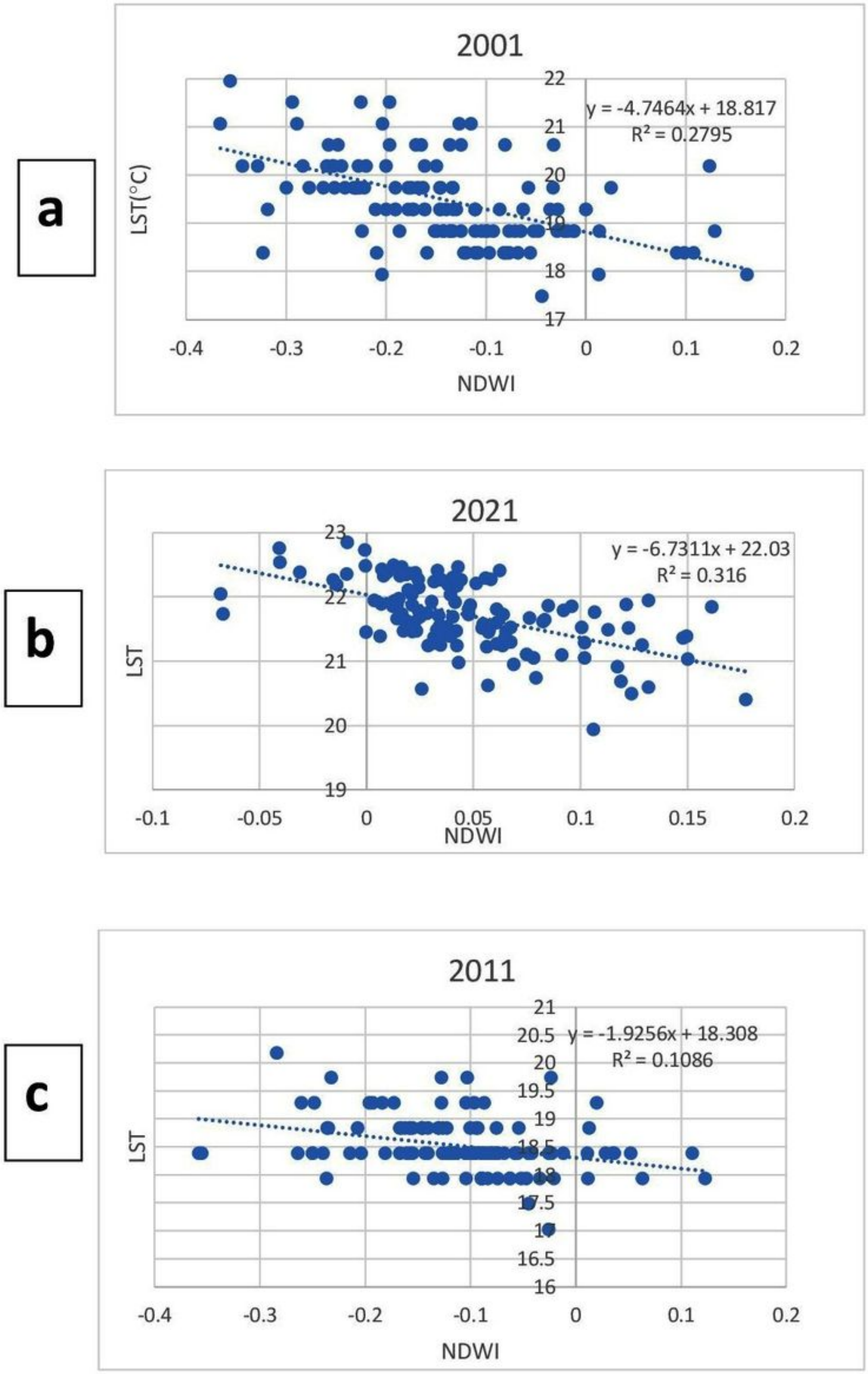

Figure 8

Regression correlation between LST and NDWI